

Kim Malin Lakeit

# Determination of Power Train Losses of a Battery Electrical Vehicle with Variation of the Outside Temperature

Bachelor's thesis  
Double Degree Energy Technology

2019



South-Eastern Finland  
University of Applied Sciences

<b>Author</b>	<b>Degree</b>	<b>Time</b>
Kim Malin Lakeit	Bachelor of Engineering	January 2019
<b>Thesis title</b>		
Determination of Power Train Losses of a Battery Electrical Vehicle with Variation of the Outside Temperature		46 pages 3 pages of appendices
<b>Commissioned by</b>		
Audi AG		
<b>Supervisor</b>		
Merja Mäkelä		
<b>Abstract</b>		
<p>The objective of this thesis was to describe the dependence of the losses in power train of an electric vehicle on the ambient temperature.</p>		
<p>In the first part of this thesis, qualitative research was used to describe generally all parts of a powertrain in a BEV. Next, their temperature behaviour as known from literature was explained. After that, by means of quantitative methods, a measurement process was created. This included the equation for calculating the energy demand, measurement setup and selection of temperature set points and driving cycles. Moreover, an evaluation concept to illustrate the results was developed.</p>		
<p>The results of these measurements showed that the ambient temperature does not significantly influence components such as the e-machines. Other elements for example the transmissions are heavily depending on the component's temperature. With the increase of the ambient temperature, the losses in the transmissions are reduced.</p>		
<b>Keywords</b>		
battery electrical vehicle, measurement process, temperature, losses, transmission		

# CONTENTS

1	INTRODUCTION .....	5
1.1	Motivation .....	6
1.2	Description of components and their losses .....	8
1.3	Structure and methods .....	9
2	POWER TRAIN COMPONENTS WITH TEMPERATURE DEPENDENCIES .....	11
2.1	Topology .....	11
2.2	Battery .....	12
2.3	Power electronics .....	13
2.4	Electric machine .....	15
2.5	Transmission .....	17
2.6	Wheel bearing.....	19
2.7	Wheel and tyre.....	22
2.8	Auxiliary system.....	24
3	ENERGY DEMAND OF A DRIVING VEHICLE .....	26
4	TEST PREPARATION.....	30
4.1	Setup of the test bench.....	30
4.2	Measurement technology .....	31
4.3	Measurement planning .....	32
4.3.1	WLTC.....	33
4.3.2	Constant speed.....	34
4.3.3	Drag mode .....	34
5	ANALYSIS OF THE RESULTS .....	37
5.1	Evaluation of the data .....	37
5.1.1	Stationary state.....	38
5.1.2	Drag mode .....	38
5.1.3	Steady-state temperatures.....	42
5.1.4	Unsteady state – WLTC.....	42

5.1.5	Impact of auxiliary systems on the driving range .....	42
5.2	Impact on the driving range .....	43
5.3	Description of errors .....	43
6	SUMMARY AND OUTLOOK .....	45
7	REFERENCES .....	47
	LIST OF SYMBOLS .....	49
	LIST OF FIGURES .....	50
	APPENDICES.....	51
	Appendix 1. Test Preparation	
	Appendix 2. Evaluation of the data	

## 1 INTRODUCTION

Rising global demand for energy and climate change have increased the calls for more environmentally friendly passenger transport in recent years. Alongside with improving the technology of combustion cars, alternative engines such as electric or hybrid vehicles gain in importance. Germany's target ,for example, was to bring one million electric cars onto the German roads by 2020 [5] in order to be able to meet its self-imposed targets of reducing greenhouse gas emissions by 40 % in 2025 compared to 1990 levels [6]. This target will be missed despite measures such as a purchase grant for electric vehicles, the expansion of the charging infrastructure, and a public procurement program for the purchase of electric vehicles by public authorities[1].

In the public discussion, the low acceptance of electric cars among the population, which is mainly caused by the limitations or changes that bring the transition to the electric car, is overall present. While examining the results of relevant surveys in more detail, in addition to the high price compared to conventional vehicles of the same vehicle class there are two arguments against choosing an alternative power train as the type of engine: the insufficient driving range and an inadequate charging duration[9]. [3]

The increasing introduction of fleet legislation in different countries places high demands on the development of new vehicles for the car manufacturers worldwide. The laws are characterized by the fact that not individual vehicles but the totality of the vehicles which were newly registered within a calendar year in each country of the manufacturer or importer must reach a certain CO<sub>2</sub> target value. Deviating from this, the fleet of one model year is used in the USA. Missing a target means a penalty payment or, as in the US, is even punished as a misdemeanour by civil action. In addition to financial disadvantages, missing a target also entails a considerable image loss. [16]

These reasons lead to a high motivation among automobile manufacturers to increase the number of state-of-the-art electric vehicles in their own product portfolio. Especially for premium manufacturers, which sell many large

vehicles with optional equipment, a large share of sold BEV<sup>1</sup>s is essential to compensate the high CO<sub>2</sub> values of the luxury class vehicles in order to be still able to achieve the fleet targets. In order to further improve the sales argument “driving range” in the evolution of the following fully electric models, potentials are now being developed on an example car of the contract company.

### **1.1 Motivation**

The ambient conditions in type approval are very specific. The automotive industry, therefore, knows much about their cars at the operating points for precisely these conditions. The temperatures at which the approval cycles for passenger cars are driven, are rather rare in reality. In Europe, for example, it is usually colder than 23 ° C at which the approval is carried out.

Consequently, there is a difference between the driving range given according to official papers and the real range. Tesla, for example, as one of the most popular manufacturers in the industry, gives on its website the ability to calculate the real range of personal driving behaviour.

As shown in Figure 1 and 2, a change of the outside temperature by 30 °C can make a range reduction of up to 34 miles or more than 50 km. [22]

---

<sup>1</sup> BEV: Battery Electrical Vehicle

## Range per Charge



Figure 1. Driving range per charge at -10 °C, calculator by Tesla [22]

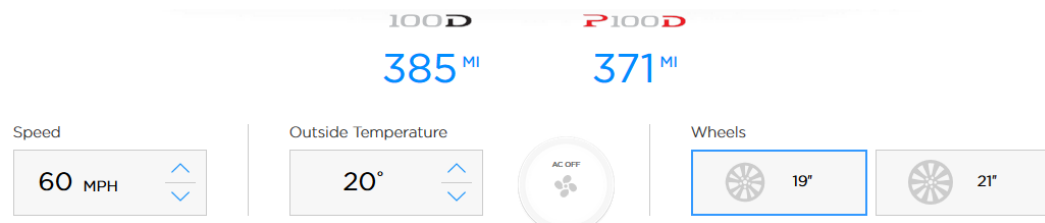


Figure 2. Driving range per charge at 20 °C, calculator by Tesla [22]

With conventional drives, the outside temperature has hardly any influence except when starting. The motors have the optimal operating points at high temperatures. The BEVs pose new questions concerning the optimal operating point of the electric machines. It must be defined if this fits with the interpretation or requirement in the development process.

Combustion produces a great amount of waste heat. This can be used to heat the passenger cabin. Cooling at high outdoor temperatures also requires energy, but this has a minor impact in comparison to heating. In the electric car, however, the influence of the outside temperature is much higher. The electric motors hardly produce any waste heat and are even cooled so as not to exceed the optimum operating temperature.

The battery is also subject to boundary conditions and can thus be operated optimally only in a certain temperature range. That is why it is necessary to provide heat energy by means of heating elements or, as with electric machines, a cooling system. These energy flows are in the case of the electric drive no 'waste products' and thus have a direct impact on the range. Moreover, the batteries nowadays are quite heavy since their energy density

compared to conventional energy sources is low. A comparison with a conventional vehicle of the same vehicle class (Q5) results in a difference in weight by half a tonne. Due to their heavy weight, electric vehicles need more energy to accelerate. Without any great success in the development of the battery technology, the driving range cannot be more improved by larger batteries. Therefore, it is necessary to find other ways to improve the driving range. The best way would be to make better use of the energy available. This means reducing any kinds of losses. The powertrain losses in a BEV should, therefore, be considered in more detail in this thesis. In this study, the concept of powertrain will include every energy flow from the battery's output to the rolling tire on the road.

The significant question examined in this thesis gives answers to the behaviour of the individual powertrain components at different temperatures.

## **1.2 Description of components and their losses**

This chapter gives a brief overview on which components comprise the powertrain. Figure 2 provides an overview of components which cause losses in both a BEV and an ICEV<sup>2</sup>. The losses in the BEV are composed of the losses along the drive train and the driving resistances (shown in Figure 3/left). In ICEV, however, much of the energy is already lost in the form of heat during the combustion process (shown in Figure 3/right). However, the losses in the BEV occur here as well, so that with the same amount of chemical energy a much smaller part of the energy remains for the kinematic energy.

---

<sup>2</sup> ICEV = Internal Combustion Engine Vehicle

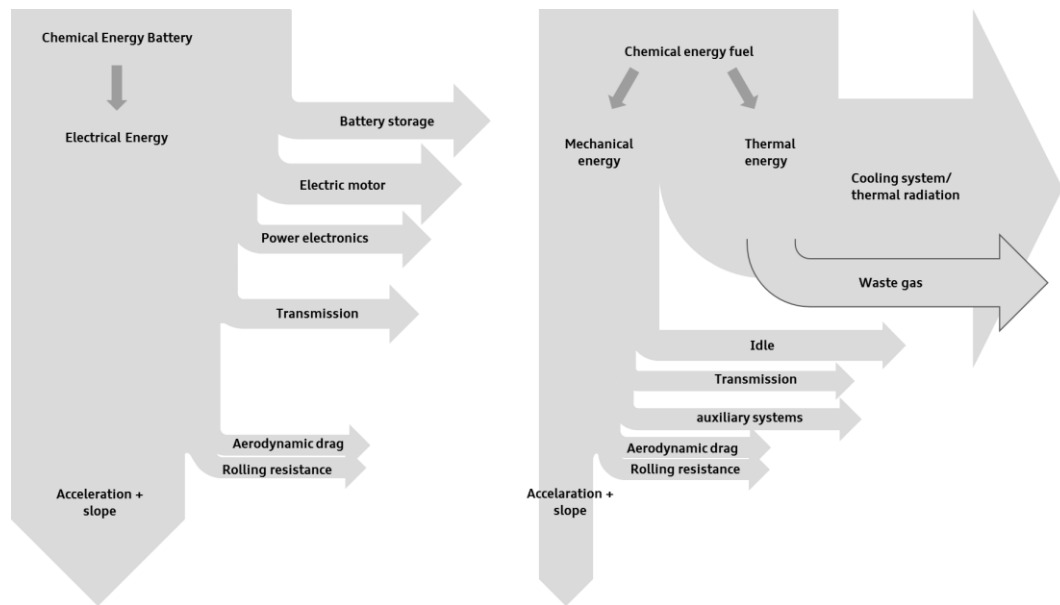


Figure 3. Comparison losses in the powertrain of a ICEV and a BEV (own diagram based on [15])

The essential component in the powertrain of electric vehicles is the electric machine or electric motor. Electric motors convert electrical energy into mechanical energy during engine operation. In generator mode, they can reverse the mechanical energy into electrical energy. Thereby, recovered braking energy is used to reduce consumption and thus range extension. In order to store the drive energy, the gas tank is replaced by an accumulator, usually called battery. Even though the accumulator is part of the powertrain, it is normally considered as a separate component, consequently it is not studied further in this study.

The power electronics control, form and switch electrical power. In motor operation, direct current is converted to alternating current.

For most current electric vehicles, a transmission with fixed ratio and axle differential is installed between the engine and the wheel. The purpose of a transmission is to convert the torque and the speed of electric motor to the needs of the drive wheels. The transmission brings the power of the engine from a high speed to a lower speed of the wheels. The use of an axle differential allows the drive wheels to rotate at different speeds during cornering. [8]

### 1.3 Structure and methods

The components of the powertrain of a BEV are described. The focus is on depicting the dependence on temperature. Subsequently, the specification of

each component in an example vehicle will be described. Various measurements were carried out on this vehicle in the course of this study. In order to achieve the objective of the thesis and to consider the friction-dependent losses of the drive train in relation to the outside temperature, a comparison of the energy requirements when driving at different speeds must be made. For this purpose, the description of this energy requirement of the components is supplemented by the driving resistances in Chapter 3. In Chapter 4, a measurement setup and the associated measurement planning is developed. This means that the structure of the test bench and the measuring technology used are described, and then the selection of the test variables temperature and speed is justified. In Chapter 5, an evaluation of the measurement results will be concluded. The results which were developed in the stationary state are further specified and then transferred or extended to dynamic driving curves.

The chapter concludes with the classification of the results based on a comparison with each other as the specific parameter driving range. In addition, a brief consideration of the measurement errors and inaccuracies will be given in Chapter 5.2. In Chapter 6, an existing thermal model of the transmission is changed, and the findings from the measurements are incorporated.

The thesis concludes with a summary and outlook on the application of results in the development of new BEVs.

## **2 POWER TRAIN COMPONENTS WITH TEMPERATURE DEPENDENCIES**

This chapter will specify the function and structure of the components of an electric power train in general as described in literature. Furthermore, it will explain the dependency on the outside temperature. Finally, the characteristics of the sample vehicle will be defined for each component.

### **2.1 Topology**

The use of electrical machines for the vehicle drive allows a variety of different design options in the arrangement of the components. In order to use as much as possible of the energy stored in the battery for the drive, it is necessary to develop space, weight and efficiency potential and to select the drive train topology in such way that in addition to the range also features such as driving dynamics, cornering, traction control or design or brand identity meet the requirements. While one combustion engine cannot be supplemented by a second engine, several electric machines can be used simultaneously. In the simplest case, one machine is used each on the front and rear axles, but using one for each wheel is also possible. This allows, among other things, the elimination of the cardan shaft in the middle of the vehicle. This affects, for example, the space available in the interior. However, several electric machines and thus several transmissions inevitably mean more losses due to friction and heat input. The e-machines can usually provide high torque over almost the entire speed range, so transmissions with fewer stages or gears, with fixed ratio or even gearless direct drives can be used. The elimination of several components compared to the ICE drive reduces losses and inertia and therefore increases the efficiency considerably. Added to this are the very high efficiencies of the components for example the electrical machines with benchmarks of 87 % to 95 %. [24]

The sample vehicle has one electric machine on both the front and rear axles. The distribution of the drive and recuperation torques to the two drive units is controlled by an engine control unit. For this purpose, the engine control unit receives torque targets from other control units in order to always be able to distribute the needed drive and recuperation torques. It also takes the traction and driving dynamics into account. Simulation calculations of the drive

showed that the priority transmission of the drive torque at the rear axle brings advantages to the overall efficiency of the drive. [2]

In addition to the e-machines, there is a gearbox on each axel and power electronics for controlling current and voltage for the e-machines. The remaining structure of the BEV is essentially no different from that of a conventional vehicle. Figure 4 shows schematically the structure of the example vehicle.

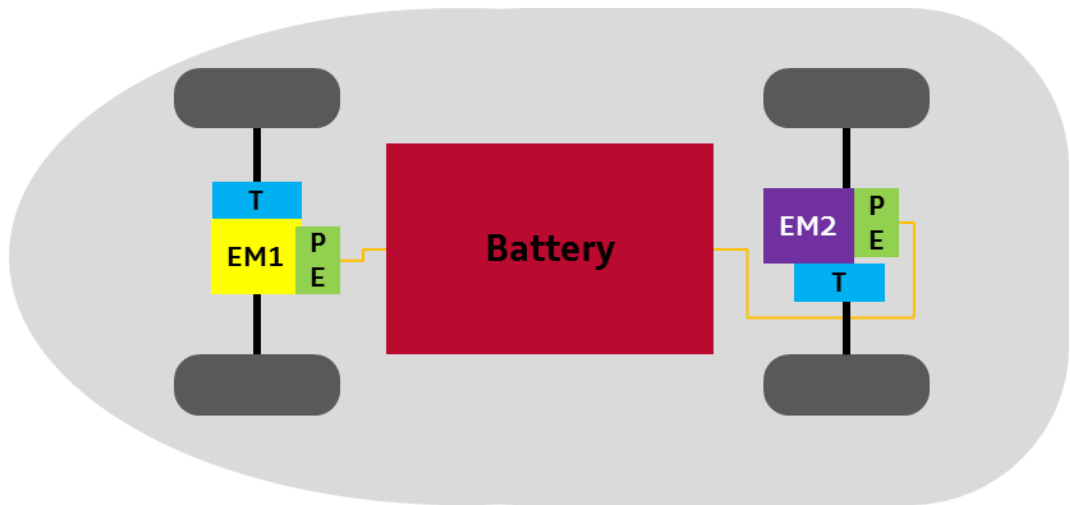


Figure 4. Illustration of the topology

The rear electric motor (EM2) sits slightly offset to the wheels. That is why a coaxial transmission is used here. On the front axle are wheels, electric motor (EM1) and transmission in a line. Here an axially parallel transmission is used. In the middle of the underbody of the vehicle, the battery is installed. In the following section, the individual components are described.

## 2.2 Battery

In addition to the electrical machine and power electronics, the battery is one part of the unique technology in BEVs. The battery<sup>3</sup> can store electrical energy as chemical energy and then release it as needed. Due to their excellent power and energy density and high cell voltage compared to other battery technologies, most electric vehicles currently use a lithium-ion battery. This

<sup>3</sup> The correct technical name for this energy storage is "accumulator", because it is rechargeable. In the language usage, however, the term "battery" has prevailed.

type of battery must always be operated with an electronic protection circuit to avoid, on the one hand, voltage areas that may damage the material and, on the other hand, temperature ranges in which for example thermal runaway could occur. In the sample vehicle the high-voltage battery is bolted in the middle under the vehicle as a chassis component. It has an energy content of 95 kWh and a peak power of 265 kW. [2]

In general, batteries have a rather high thermal mass, why temperature changes take a long time to make an impact at all. Nevertheless, the operating temperature is normally between  $-30\text{ }^{\circ}\text{C}$  and  $+60\text{ }^{\circ}\text{C}$ . The optimum power range is between  $15\text{ }^{\circ}\text{C}$  and  $35\text{ }^{\circ}\text{C}$ . As shown in Figure 5 before and after the temperature window, the power limit decreases.

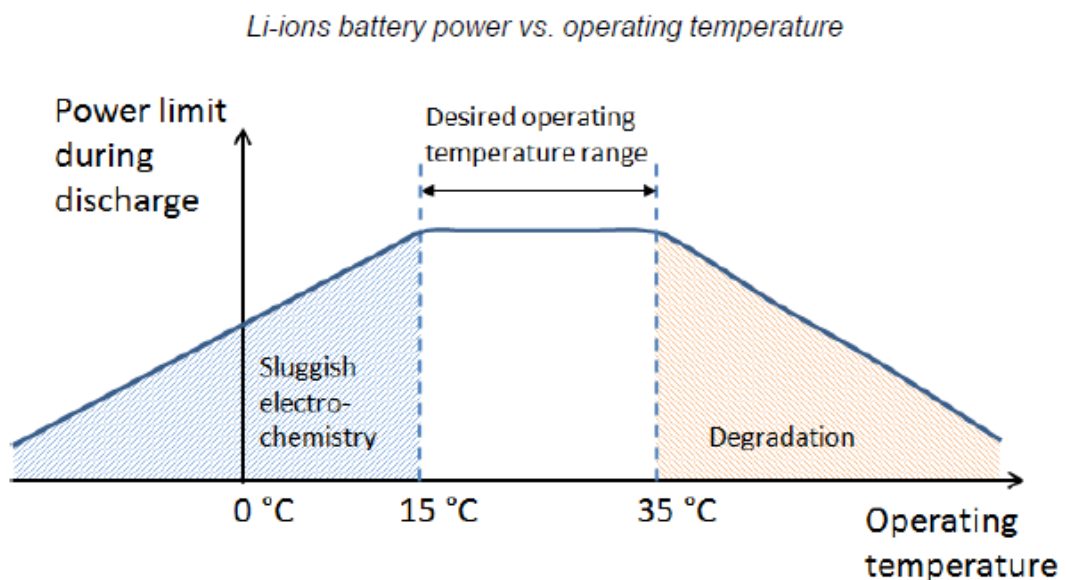


Figure 5. Operating temperature of a lithium ions battery [4]

In order to achieve this temperature, the battery has a coolant circuit and a heating element. As a result, the performance and thus the losses of the battery are little or not dependent on the outside temperature. [14]

Of course, the operation of this thermo system affects the available driving range, but these relationships are not considered further in this thesis.

### 2.3 Power electronics

In general, the task of power electronic is to switch, control and transform electrical energy with the help of electronic components. In electrical drive technology, power distribution, electrochemistry and electrical heat, power electronics are being used to an increasing extent. [11]

In vehicle technology, power electronics generally describe the control unit for the electric drive. In order to produce a rotating field in a three-phase machine and thus a torque, a voltage or current system is required. The creation of this is the main task of the controller. Irrespective of the operating voltage and rated power, the topology of a bridge circuit can be used as an inverter, as shown in Figure 6.

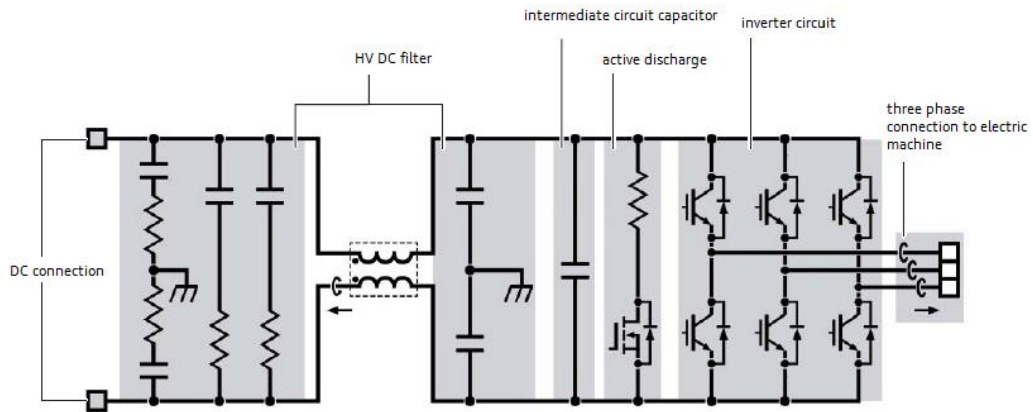


Figure 6. Bridge circuit [13]

On the left side is the connection to the HV battery. This provides DC power. Since the battery is vulnerable to EMI noise, a filter is switched between the actual converter circuit and the battery connection. The right part of the figure shows six semiconductor switching modules divided into three pairs, each supplying one phase of the electric motor. While the battery is being charged or in recuperation phase, the power electronics function as a DC/DC converter.

The 12V on-board electrical system in BEVs is in most cases also supplied via the high-voltage system. The generator, which converts the mechanical into electrical energy in ICEVs, is therefore eliminated and replaced by a DC/DC converter. Each e-machine requires its own control unit. Accordingly, the sample vehicle has on the front and the rear axle a power electronics component. The power electronics are screwed directly to the e-machine and contacted electrically via three phases. The losses in the power electronics consist of passage and switching losses. The switching losses are composed of the switching frequency and the required switching energy. These are thus dependent on current and voltage, but not on the temperature. [13]

The forward losses are related to diode resistance and amperage. The resistance depends on the temperature. The higher the temperature of the

diode, the higher the losses. That is why the power electronics are connected to the cooling system of the electric machines. The cooling water flows from the power electronics via the cooling water nozzles into the electric motor. Due to the very small size of the chips and their material properties, they have no high heat capacity and react even to small temperature fluctuations with large changes in the loss behaviour. In principle, the colder the chips and the smaller the phase current, the smaller the losses. [13]

The losses within the power electronics are mainly dependent on current and voltage but little on the temperature, especially since this varies little through the cooling circuit. In addition, the scale of the losses recorded here is rather small compared to other components and can be seen as insignificant. [13]

## 2.4 Electric machine

Electric machines convert electrical energy into mechanical energy and vice versa. The direction of energy flow is reversible and depending on the direction the machine operates in the motor or generator mode. In electric vehicles, the braking energy can thus be recovered in generator mode. This process is called recuperation. [24]

Nowadays, there is a variety of electric drive machines - such as DC machines, permanent magnet synchronous machines (PSM), foreign excitation synchronous machines (FSM), asynchronous machines (ASM) and switched reluctance machines (SRM). Due to the simple design, high reliability and thus an almost maintenance-free operation, as well as high efficiencies, nowadays almost exclusively three-phase machines are used as electric drives. These consist of a stationary part, also called 'stator', and a rotating part, called 'rotor'. In the case of an asynchronous machine, the rotor consists of a ferromagnetic cylinder. [24]

There are three types of losses in these e-machines:

- Electrical losses in the winding of the machine
- Magnetic losses composed of hysteresis and eddy current losses
- friction and mechanical losses.

The electrical losses result from ohmic resistance  $R$  and current  $I$  squared.

$$P_{loss,electrical} = R * I^2$$

The current in the winding and thus also the electrical losses grow with increasing speed.

In addition to stator, rotor and closing bearings, there are no other parts that move. Thus, losses caused by mechanical friction are very low.

Nevertheless, the stator, rotor and bearings are heating up in operation. This heat input causes some losses. [13] In the example vehicle, the electric machines are liquid-cooled on the front and rear axles. Both the stator and the rotor are flowed through with coolant, shown in Figure 7 as the blue areas.

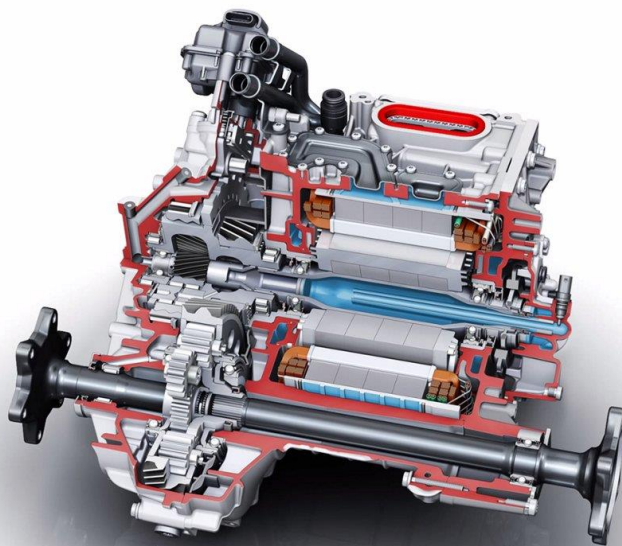


Figure 7. Sectional view electric machine front axle [2]

The additional internal rotor cooling results in significant advantages in terms of continuous power and reproducible peak power. The coolant also passes through the power electronics. Of course, the same as with the battery, the operation of the cooling system reduces the range because these systems require some power to operate the pumps and heat exchanger. In contrast to the battery, however, the window of the operating temperature is significantly larger, so that there are different operating temperatures depending on the outside temperature. A change in the outside temperature has therefore a small effect on the losses. However, these relationships will not be part of this thesis. Instead, the focus is on the steady-state temperatures of the electric machines.

In order to be able to classify the loss behaviour of the electric machines at different speeds, it is necessary to look at the torque output curve. While with ICEV the maximum torque is available only after a certain speed, with an asynchronous machine the maximum torque can be delivered from the first turn. This maximum torque is limited only by the maximum permissible current.

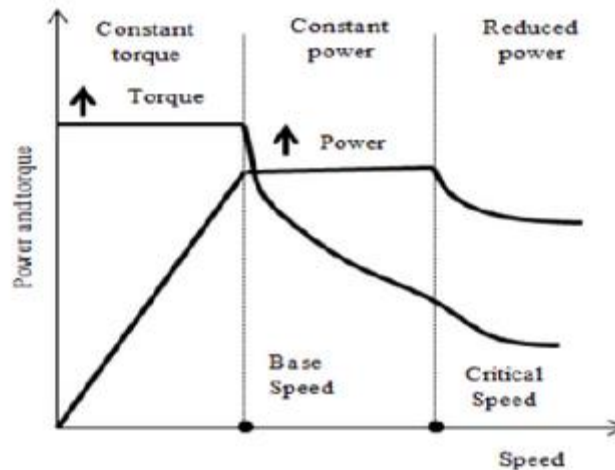


Figure 8. Speed-torque characteristics of an ASM motor [21]

In Figure 8, it can be seen that the power curve continues to go up with increasing speed. With a certain speed, the power can be maintained by a field weakening which reduces the torque. In order to always provide exactly the required speed and torque at the wheels despite this behaviour, transmissions are used. This will be described in more detail below.

## 2.5 Transmission

Gearboxes are mechanical systems for converting and transmitting motions and forces. [11] Since the electric machines in an electric vehicle are capable of covering the entire speed and torque range, in contrast to ICEVs, transmissions with many different gears are not necessary. In many of the past series of electric vehicles, an input gearbox with differential is used. In some cases, multi-speed transmissions are used [12] since these enable optimized operation in terms of efficiency, comfort or driving performance.

The following types of losses can occur in a transmission:

- Sliding and rolling friction losses in the gear wheels and the bearings

- Splash and ventilation losses of the gear wheels
- Losses in the shaft and bearing seals
- Losses caused by the use of a clutch

More gears mean greater losses due to more moving parts creating friction in the wheels. [24] With a single-stage gearbox, fewer moving parts are used, but the single gears must transmit higher forces. This means that a stable design with large gears and strong bearings is necessary.

The mechanical friction losses can be reduced for example by lubrication with oil. In order to set this oil in motion right at the start of the operation, some forces are required that are reflected in losses in the overall energy balance. Nevertheless, lubrication is also a common procedure for reducing abrasion. The losses due to the shear forces are directly related to the viscosity of the lubricant:

$$\tau = \eta * \dot{\gamma} \quad 2.2$$

According to the Newtonian law of viscosity, the shear stress  $\tau$  in a laminar flow process is proportionally dependent on the shear rate  $\dot{\gamma}$ . The proportionality constant  $\eta$  is referred to as dynamic viscosity. This decreases with increasing temperature, so that the thrust is also lower. This temperature dependence can be expressed via the Andrade equation:

$$\eta = A * e^{\frac{b}{T}} \quad 2.3$$

This describes the dynamic viscosity  $\eta$  as a linear relationship in dependence to the absolute temperature  $T$ . The constants  $b$  and  $A$  are dependent on the fluid used.

Because of the smaller number of parts, less friction losses occur in a single-stage transmission. This results in less heat power for warming up the oil.

Therefore, the losses of these transmission types might be lower at a steady-state temperature but higher in the warm-up phase.

It cannot be determined which type of transmission has overall the better energy balance.

The example vehicle has different transmissions on the front and rear axles. Both have only one gear.

The transmission of the front axle is a two-stage axis parallel transmission as

shown on the left in Figure 9. The first stage is a planetary gear. The second stage a simple spur gear which serves as a differential.

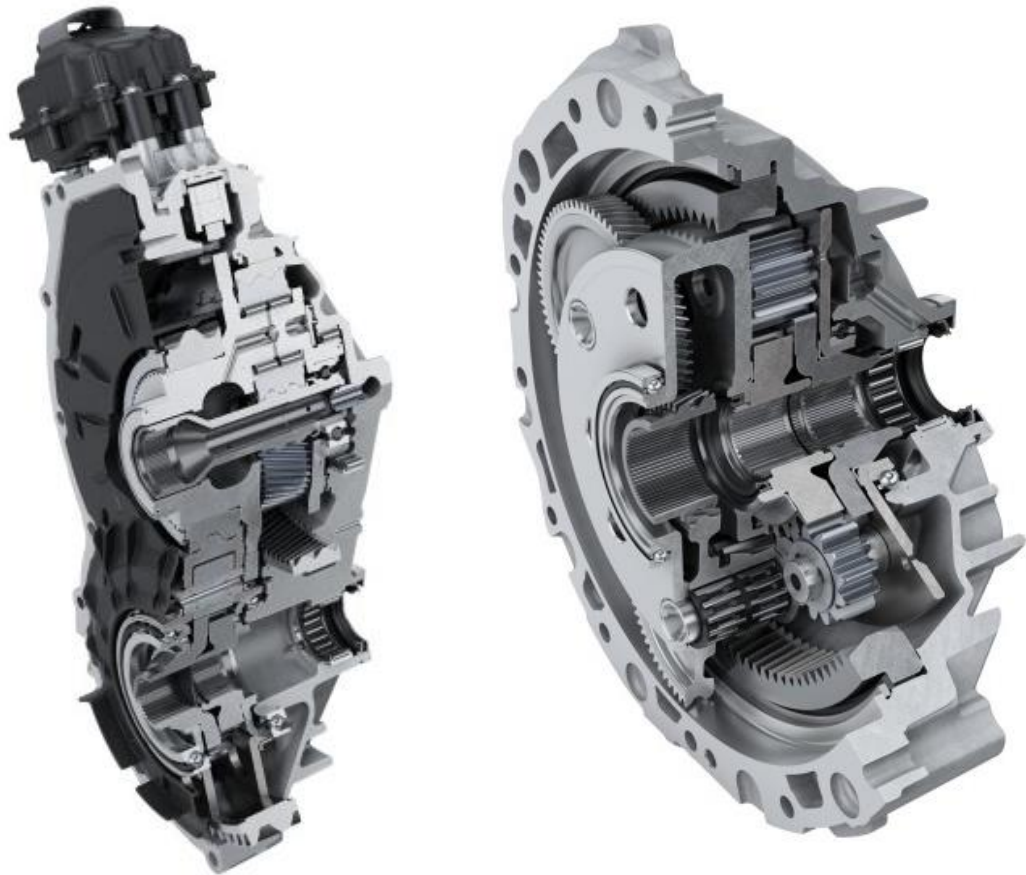


Figure 9. Sectional view of the axis parallel (left) and coaxial (right) transmission of the sample vehicle [18]

On the rear axle, however, there is a coaxial transmission, which consists of only one stage. This is also realized by a planetary gear and shown on the right. It is a crucial part of this thesis to define which type transmission has the lower losses depending on the temperature. In Chapter 5, the losses in total and per axis will be determined and analysed.

## 2.6 Wheel bearing

The wheel suspension's components wheel carrier, wheel bearing, handlebar (with kinematic pairs and rubber bearings), spring and damper are in charge of the adjustment of the wheels and provide support against external forces. [17] In BEVs these components hardly differ from ICEV's in functionality, structure and materials.

Generally, most of these components do not significantly affect the vehicle's consumption or the powertrain resistance. In any case, their influence can be

considered independent of temperature. The losses in wheel bearings, however, are very much dependent on the outside temperature. The task of the wheel bearings is to direct and support the shafts and axles. They connect the wheel hub to the wheel carrier and absorb all the axial and radial forces introduced by the tyres into the frame [23]. Radial forces are circumferential forces generated by the rotational movement. They act at right angles to the longitudinal axis on the wheel bearing. In contrast, axial forces act on the wheel bearing in the direction of the longitudinal axis. They arise, for example, while driving along curves.

Today, most passenger cars use double-row angular contact ball bearing units with an undivided outer ring and one or two separate inner rings. Depending on the degree of integration of functions in the inner or outer ring, these bearings are called wheel bearings of 1st, 2nd or 3rd generation. By combining the outer ring into one unit, it is possible to seal the lubrication of the ball bearings so that they are maintained over the entire life cycle of the vehicle, and sensors such as the encoder for the ABS can be integrated.

Figure 10 shows typical examples of wheel bearing units of different generations.



Figure 10. The different generations of wheel bearings [7]

The losses occurring in the wheel bearing can be well represented by friction torque. The friction in the bearing is caused by the resistance between rolling elements and raceways, by the resistance of the lubricant and by the grinding

of the seal in sealed bearings. The friction torque  $M_{fr}$  depends on the bearing load, the lubrication state and the speed. It can approximately be calculated from the friction coefficient  $\mu_{wb}$ , the diameter of the inner ring  $d_{wb}$ , and the resulting bearing load  $F$ :

$$M_{fr} = \mu_{wb} * F * d_{wb} / 2$$

2.4

The friction coefficient  $\mu_{wb}$  is mainly dependent on the seal and the lubricant in the ball race. The viscosity of the lubricant is heavily influenced by the outside temperature. The relationship between viscosity and temperature has already been described in Chapter 2.5 and should be applied here as well.

This affects the friction torque especially at the beginning of a ride, but also in the warm-up, stationary state.

The sample vehicle has wheel bearings of the second generation which are fastened by screwing on the swirl bearing and the wheel hub. Figure 11 shows this example in a similar vehicle.

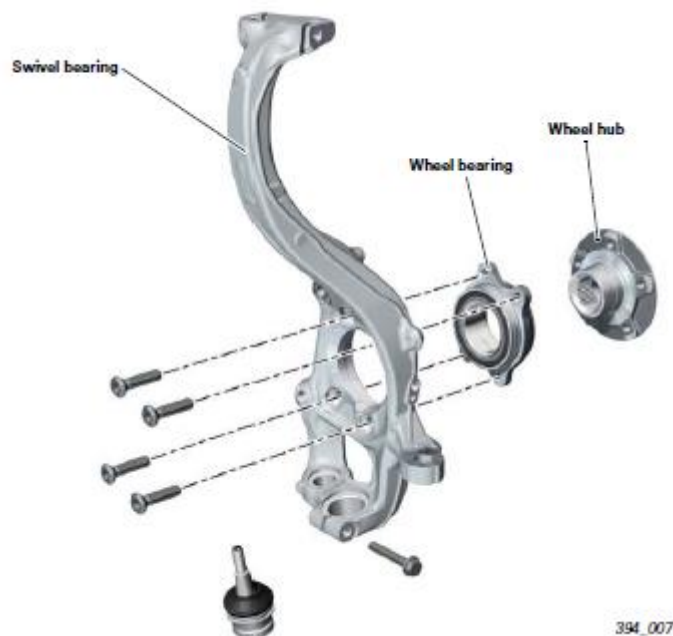


Figure 11. Exploded view of a wheel carrier [2]

Figure 12 shows some measurements of the TU Brunswick on discrete wheel bearings of the same kind. The green line is the ambient temperature. The red and blue line are the temperatures of the bearing. The line in the upper part of

the figure shows the losses occurring in the steady state, without any warm-up effects.

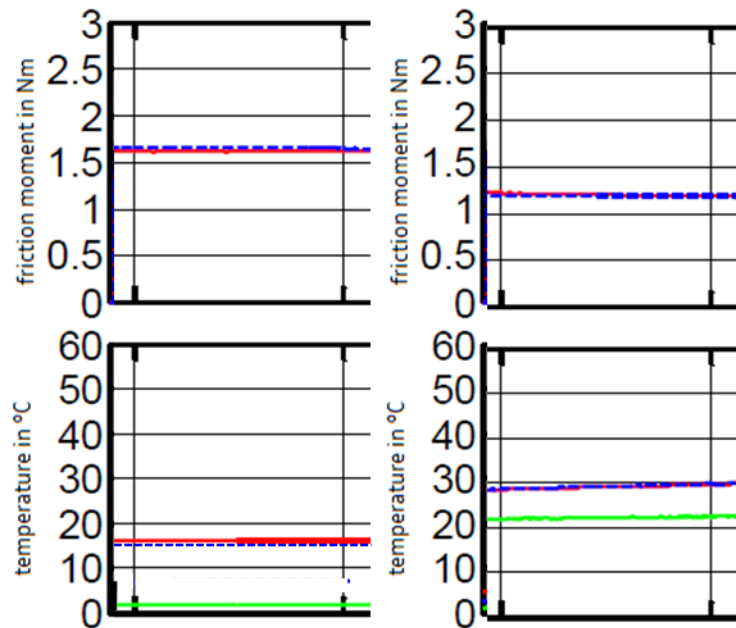


Figure 12. Friction moment of a wheel bearing at 0 °C and 20 °C ambient temperature [19]

At 0 °C, the friction torque is about 40 % higher than in the warmer surrounding. The difference between the ambient and the wheel bearing temperature is significantly greater at 0 °C than at 20 °C. Nevertheless, for a closer study on these connections some additional measurement technology would be necessary. In order to limit the scope of this thesis and because of the similarity to ICEVs, the specific value for the sample vehicle used will not be measured but transferred or averaged.

## 2.7 Wheel and tyre

As a link between the road and the vehicle, tyres play a key role in driving behaviour. The tyre is attached to the vehicle via a rim on the wheel suspension (described in chapter 2.6).

A modern vehicle tyre is a technologically sophisticated component whose properties can be adjusted specifically. When selecting the tyre parameters, a distinction is made between the criteria of comfort, environmental compatibility, economic and driving safety. Depending on the tyre model and the area of application, there are different aspects against which the driving characteristics can be adjusted.[20] The wheel resistance  $F_{rr}$  is composed of all forces which occur in the wheel and the suspension. These include:

- Rolling resistance of the tyre
- Losses caused by the road surface
- Losses due to skew
- Bearing friction and residual braking torque
- Gearbox and differential resistance. [20]

The losses in wheel bearings and transmission have already been described in the previous chapters. Since differences in the road surface and losses due to skew are eliminated in a test bench, only the rolling resistance parameter  $f_{rr}$  will be considered in more detail below.

The rolling resistance coefficient depends on different parameters. In addition to the dependence on the filling pressure, the coefficient depends on the load of the wheel. Nevertheless, the changes caused by the load are negligible in the range of standard speeds. In BEVs owing to the battery, the vehicle weight is higher than that of vehicles with an internal combustion engine. This results in a higher rolling resistance. In the series of measurements made for this study, the vehicle weight does not change, so this dependency does not have to be considered. The tyre inflation pressure was set to norm conditions. The amount of air in the tyre remains constant throughout all measurements, but the pressure changes depending on the outside temperature. Accordingly, the rolling resistance coefficient is dependent on the outside temperature, or rather, the tyre temperature. In general, it can be said that the warmer the vehicle tyre, the lower its rolling resistance. Tests carried out by Michelin on a tyre dynamometer have shown that in the temperature range from 10 °C to 40 °C the rolling resistance force drops by 0.6 % per degree Celsius as shown in Figure 13. [20]

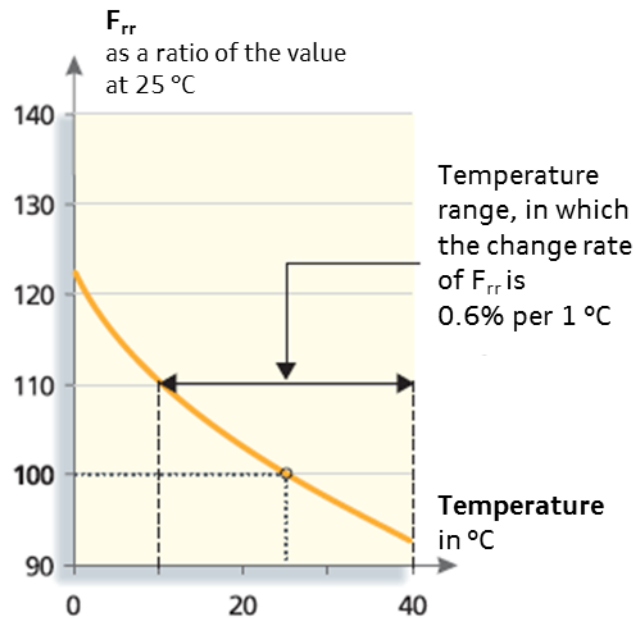


Figure 13. Rolling resistance depending on the ambient temperature, own translation of [20, p. 86]

The significant reason for the increase in rolling resistance as a result of a reduction in temperature is the tyre rubber. The reduced temperature causes a hardening of the material with altered spring-damper properties. Based on these rates of change the effects of the test room temperature on the rolling resistance were calculated. The temperature ranges which are not covered here are extrapolated. [20]

## 2.8 Auxiliary system

The components of a vehicle which are not directly responsible for the drive are called auxiliary consumers. In addition to assistance systems such as parking sensors or thermal management systems for battery and e-machine, these can also be comfort functions, such as a multimedia-system. [25]

The vehicle's main auxiliary consumers are for used heating, ventilation and air conditioning of the passenger cabin [25]. The energy demand of these components strongly depends on the outside temperature, but also on the comfort temperature of the passengers.

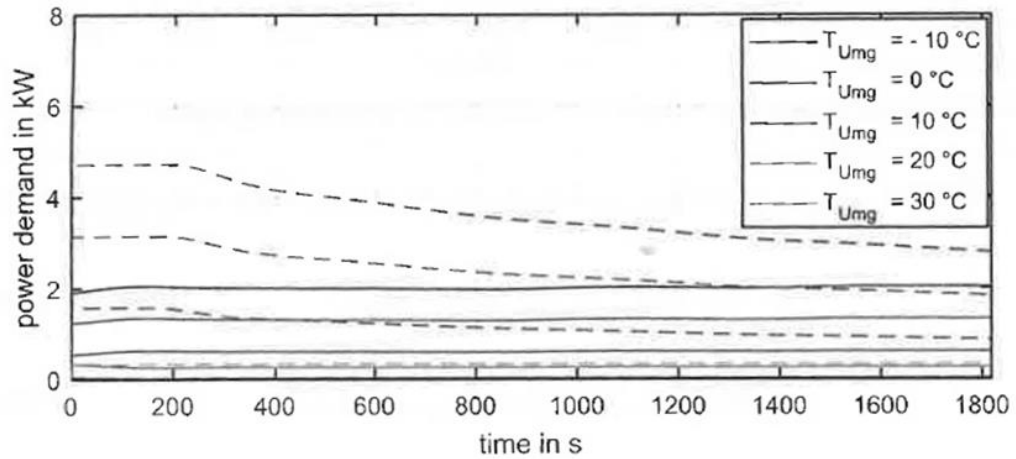


Figure 14. Power demand for the auxiliary energy flow with and without preconditioning (dashed) of the passenger cabin [25]

Figure 14 shows the power demand for heating or cooling the passenger cabin to 20 °C. The dashed lines show the demand when the cabin temperature was at ambient temperature at the beginning of the test. In this test of authors of [25] a BEV with a PTC element was used. This results in a higher energy demand for heating than for cooling.

In the example vehicle, a heat pump is installed which can reduce the energy consumption for heating by using waste heat. Overall, the energy for auxiliary users depends very much on the concept used and must be considered individually. In the context of this thesis, only the fundamental relationship between the total energy consumption of the vehicle and the use of secondary consumers should be documented.

### 3 ENERGY DEMAND OF A DRIVING VEHICLE

The energy which is needed to move the vehicle can be described by the product of tractive force  $F_{tr}$  and the covered distance  $dis$ :

$$E_{tr} = F_{tr} * dis \quad 3.1$$

The tractive force consists of the driving resistances shown in Figure 15 and the losses in the power train of the vehicle  $F_{dt}$ .

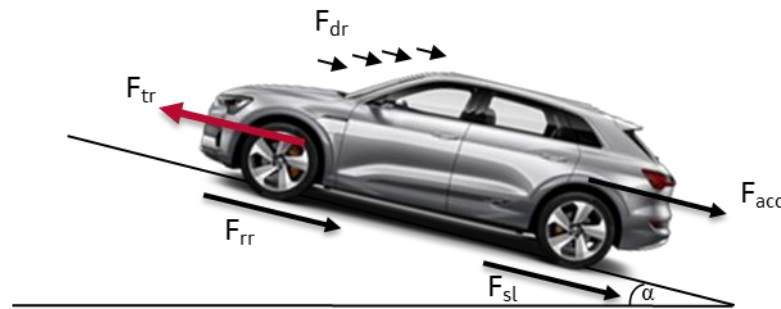


Figure 15. Driving resistances

$$F_{tr} = F_{acc} + F_{rr} + F_{dr} + F_{sl} + F_{dt} \quad 3.2$$

$F_{tr}$  describes the required force at the driven wheels. It can be divided in the components as presented below.

#### Acceleration resistance

$$F_{acc} = m_{veh-red} * a_x = m_{veh} * (1 + \varepsilon) * a_x \quad 3.3$$

“ $F_{acc}$  describes the force which is induced by longitudinal acceleration of the vehicle’s mass. The mass  $m_{veh-red}$  is the sum of the vehicle mass and the reduced rotational mass from the moment of inertia of rotating parts inside the power train.” [25] In order to simplify this variable, there is an approach of a constant factor taking the rotational mass into account. In the case of the sample vehicle,  $\varepsilon$  is set to 0.03. The acceleration force is not dependent on the ambient temperature, but only on the speed change per second as  $a_x$ .

## Rolling resistance

$$F_{rr} = f_{rr} * m_{veh} * g * \cos(\alpha) \quad 3.4$$

The rolling resistance is a function of the vehicle's mass  $m_{veh}$ , the acceleration of gravity  $g$ , the road gradient  $\alpha$  and the parameter  $f_{rr}$ . The parameter depends on the tyre configuration and road condition. As described in Chapter 2.7, this parameter depends also on the ambient temperature and, therefore, the force  $F_{rr}$  as well.

## Slope force

$$F_{sl} = m_{veh} * g * \sin(\alpha) * v_x \quad 3.5$$

The slope force  $F_{sl}$  is the downhill force, and thus the second component of the weight force in addition to the shear force in  $F_{rr}$ . [25] For measurements performed on a test bench, this value is 0 because the slope  $\alpha$  is 0.

## Aerodynamic drag

$$F_{dr} = 0.5 * A_x * c_d * \rho * v_x^2 \quad 3.6$$

The air resistance is created by a flow around and through the vehicle. It is composed of the cross-sectional area of the vehicle  $A_x$ , the air density  $\rho$ , an air resistance coefficient  $c_d$  and the flow velocity  $v_x$ . The flow velocity is equal to the driving speed of the vehicle when driving without curves and gradient, like on the test bench. [25]

Intensive development work throughout the whole car industry has significantly reduced drag coefficient in recent decades because even the smallest changes in driving resistance mean several kilometres of driving range for electric cars. The  $c_d$  value is set to 0.28 for the sample vehicle.

$$\rho = \frac{p * M}{R * T} \quad 3.7$$

The air density  $\rho$  arises from the ambient pressure  $p$ , the ambient temperature  $T$ , and the constant parameters molar mass of the air  $M$  and universal gas constant  $R$ .

Figure 16 shows this behaviour as a basic calculation example. It can be seen here that the aerodynamic driving resistance decreases with increasing temperature.

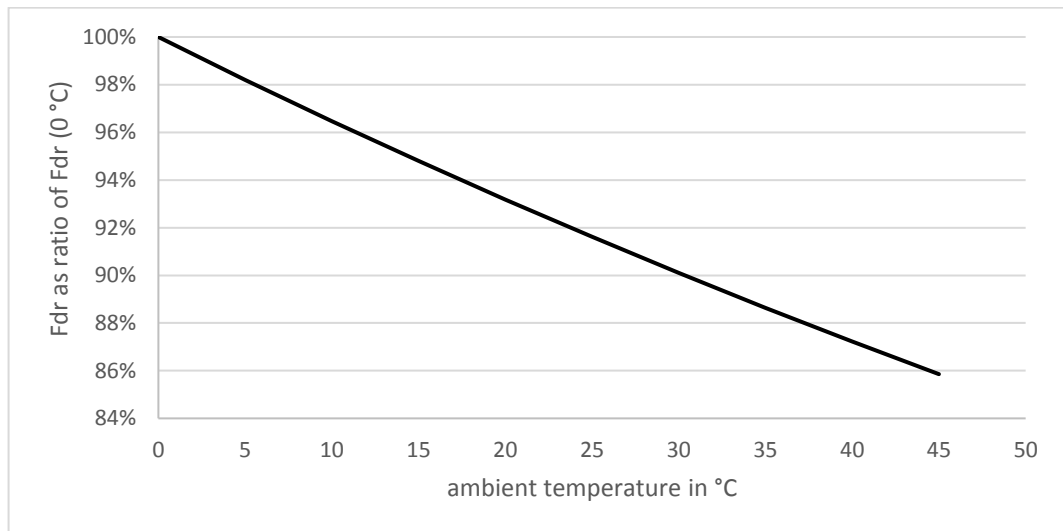


Figure 16. Aerodynamic drag  $F_{dr}$  as a function of the ambient temperature

As the speed squared enters this driving resistance, there is a great influence caused by the aerodynamics, especially at high speeds. As shown in Figure 17, the drag force is 70 % higher at 130 km/h than at 100 km/h. At 10 km/h, however,  $F_{dr}$  is only 1 % of the value at 100 km/h.

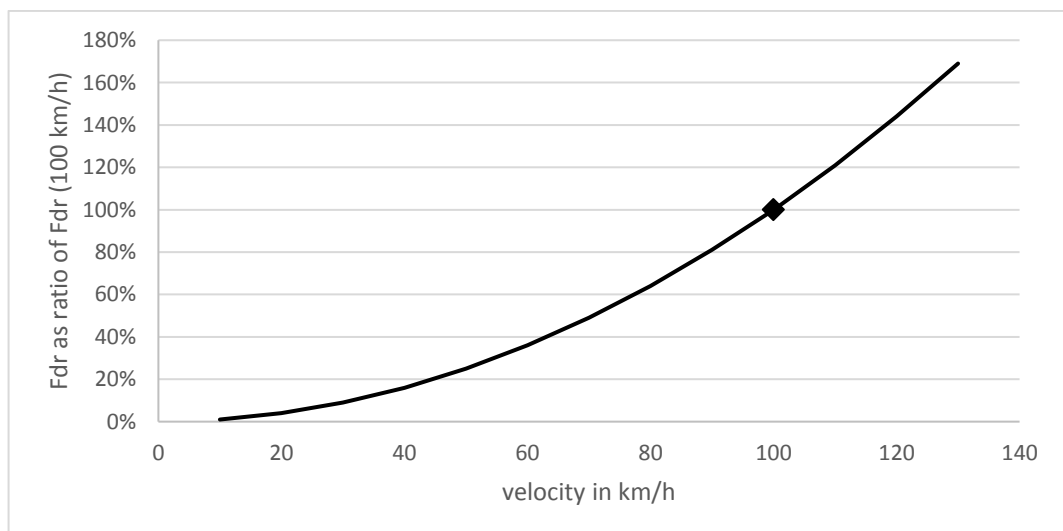


Figure 17. Aerodynamic drag  $F_{dr}$  as a function of the velocity  $v$  (basis  $v = 100$  km/h)

## Drive train losses

The losses in the powertrain  $F_{dt}$  consist of the losses in the individual components described in Chapter 2. Since these losses are usually indicated as power in Watt, in the further course of this thesis the term 'power' is used instead of forces.

$$P_{dt} = P_{EM1} + P_{EM2} + P_{transmission} + P_{wheel+tyre} \quad 3.8$$

Power can certainly be calculated in many ways.

The calculation of the translational power necessary to overcome the driving resistance is calculated by multiplying the force  $F$  with the respective velocity  $v$ .

For the electric power, the current  $I$  is multiplied by the voltage  $U$ . For the rotatory power the rotation speed and the torque are multiplied:

$$P = F * v = U * I = 2 * \pi * \frac{1}{60} * M * n \quad 3.9$$

The total energy demand CED of the measurement or a cycle thus results from the integral of the tractive power and the recuperated energy:

$$CED = \int P_{tr} - P_{rec} dt \quad 3.10$$

Since recuperation in the drive train may under certain circumstances result in a different efficiency due to the changed direction of action, these phases are excluded in the evaluations of this study. Recuperation phase can be recognized by the fact that the battery power output is negative. This means that at constant voltage the current changes its sign.

In order to further simplify the calculation, the time interval is also set to one second so that a sum can be used instead of an integral. The result for the energy demand CED in this exercise is the following equation:

$$CED = \sum_0^t P_{tr}(I_{battery} > 0, t) \quad 3.11$$

## 4 TEST PREPARATION

This chapter describes not only the structure of the test bench, but also the measuring technology used. In the last part, explanations are given for the selection of the temperatures considered and the speeds or cycles covered.

### 4.1 Setup of the test bench

All measurements for this thesis are carried out on a complete vehicle test bench in the form of a flat-bed test bench. This offers the advantage of examining the mechanical driving resistances on a level surface as shown in Figure 18 below. This means almost real rolling conditions assuming and simulating a constant aerodynamic drag. The changing air density due to the temperature was beyond the scope of this study.

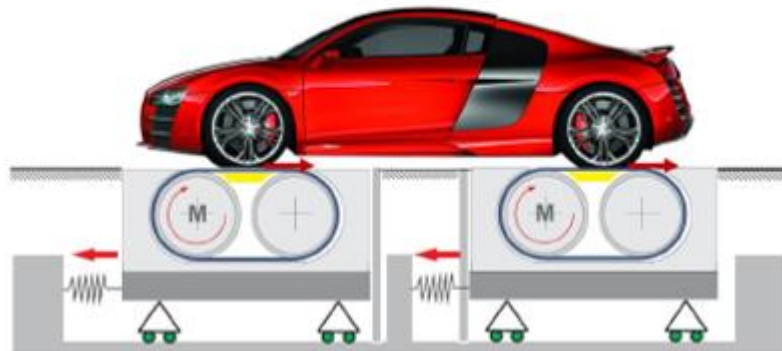


Figure 18. Schema of a flat-bed test bench

The drive and braking forces are directly measurable. The maximum achievable speed is 250 km/h. Furthermore, this dynamometer offers a high degree of dynamics since the rotational mass is lower than in the case of the standard roller test bed which are also common in the automotive industry. Ambient conditions such as temperature and humidity can be varied depending on the test specification and adjusted with the aid of a refrigeration and air conditioning system. The technical limits of  $-30\text{ }^{\circ}\text{C}$  to  $+40\text{ }^{\circ}\text{C}$  are not completely exhausted in the measurements of this study. The test bench can be operated in two different modes: either the drive power comes from the engines of the test bench, sets the belts and thus the wheels of the vehicle in motion (drag mode) or the aggregates of the vehicle drive the belts of the test bench (thrust mode)

## 4.2 Measurement technology

The selected test vehicle is a preproduction model. Nevertheless, it is similar to the vehicles that are available to the customer for purchase, in all relevant respects.

Most of the measurement quantities used in this study are measured or calculated in the vehicle for control purposes. These can be recorded during the measurement via the CAN or Flex Ray bus system. In addition, there is measuring equipment on the test bench as well as some external temperature measuring points on the vehicle that have been specially installed for this series of measurements.

Next to the belt speed and drive and braking forces of all four wheels, the measuring equipment of the test bench includes gauges for temperatures and other ambient parameters. Moreover, the speed of the airstream fan gives the velocity of the airflow for the calculation of the aerodynamic drag. Finally, with an infrared sensor, the surface temperature of the tyres is recorded on the tread.

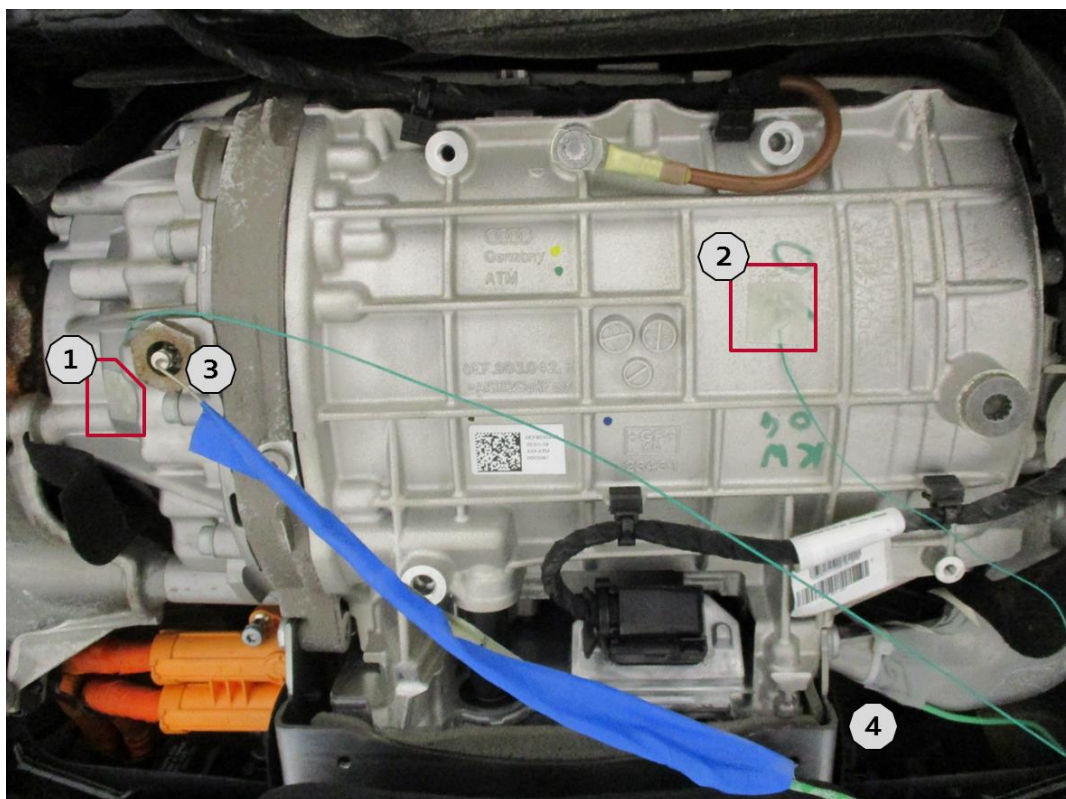


Figure 19. Measurement technology on the rear axle

Figure 19 shows the measuring technology on the rear axle. At the measuring points 1 and 2, the surface temperatures of the transmission and electric motor are recorded. Measuring point 3 detects the temperature of the

transmission oil via the drain plug. At position 4, the temperature of the ambient air in the engine compartment is measured. Thus, on the one hand, it can be monitored whether the conditions of the desired temperature have been completed or met. On the other hand, a statement about the release of heat loss to the environment can be made through this temperature monitoring process. This principle applies to the front axle as well. Because of assembly space design, the measuring points cannot be seen properly. A picture showing mainly the chassis subframe can be found in Appendix 1/1. The measured value is recorded by the test bench technology as well as the external measuring technology at 10 Hz. The measuring signals of the on-board control units are partly in a different frequency. These were then stretched or interpolated during the evaluation to the appropriate length.

### **4.3 Measurement planning**

In this thesis, the powertrain losses at different outside temperatures are investigated. Among the many possible temperature points, four temperatures were selected for organizational reasons. At these temperatures, different driving curves are considered.

The WLTP type approval cycle is already in use in Europe and will be used in more and more countries around the world to determine more realistic results in fuel consumption [10] over the next few years. The WLTP is run at 23 °C ambient temperature. [10]

In North America, the type approval of passenger cars requires a choice of five different cycles, each with specific parameters such as ambient temperature or battery state of charge. One of these tests takes place at 35 °C, another at -7 °C. In order to be able to draw conclusions from the measurements made in this study with respect to the tests in North America, these temperatures were selected.

After this selection, a large gap would have remained between -7 °C and +23 °C. However, since in large parts of Europe exactly these temperatures correspond to the annual average temperatures, another setpoint seemed reasonable here. The temperature +7 °C was picked which corresponds to the annual average temperature of Finland.

The conditioning of the test bench is done in most cases overnight, to make sure that all components have reached the ambient temperature. In a few

cases conditioning took only a few hours. As a result, not all components were completely cooled or warmed. The resulting error is discussed in chapter 5.2.

### 4.3.1 WLTC

The Worldwide Harmonized Light Vehicle Test Procedure (WLTP) is a cycle based on international data. These results in consumption values are sufficiently close to real customer consumption compared to older, widely known cycles such as the NEFC. The speed of one run is shown in Figure 20. In a full type approval test according to WLTP, several of these are driven with different charging cycles in between, depending on the design (hybrid, BEV) of the vehicle.

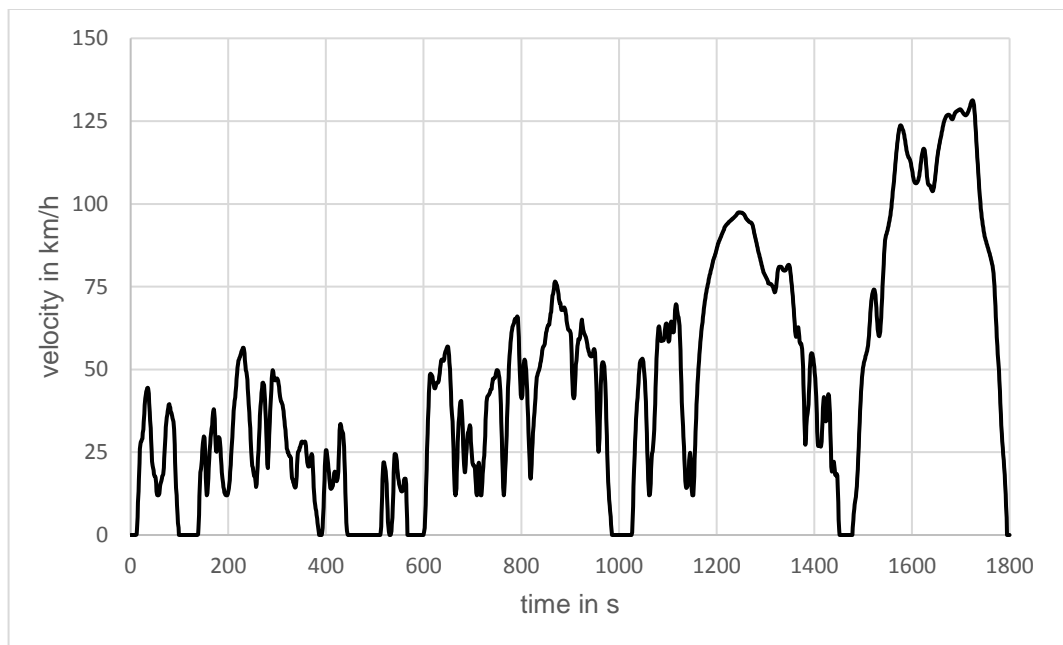


Figure 20. Driving profile of the WLTC

One WLTC consists of four phases. The first phase represents typical city traffic. The second and third phases are overland routes and the fourth and final phase simulates a highway journey with top speeds of up to 130 km/h. The total distance is 23 km with a duration of 30 minutes. This cycle is very dynamic with many acceleration and braking components.

The WLTP is very well suited for comparing the required energy since there are already many empirical values available. In this thesis, only a single WLTC will be used, never the whole procedure.

### 4.3.2 Constant speed

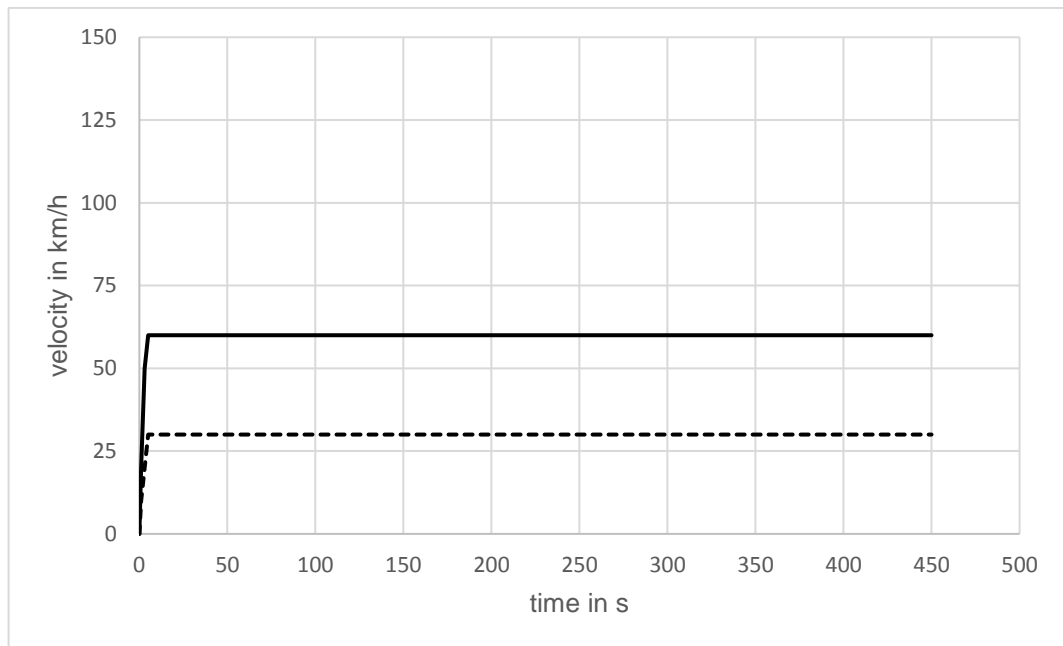


Figure 21. Driving profile at constant speed 30 km/h (dashed) and 60 km/h

In order to bring the components to a constant temperature and thus to eliminate the losses caused by heat input and to be able to name only the pure mechanical losses, tests were run at a constant speed.

Since the stationary temperatures and losses are not the same for every load, but vary depending on the speed, two different speeds were compared as shown in Figure 21.

The first selected speed is 60 km/h. The results of these measurements are compared with the losses at 30 km/h. The expectation is a lower final temperature of the components which may lead to larger losses. It is also known that the driving resistances, such as the rolling resistance, make up a larger proportion at lower speeds. [20] That should lead to higher losses compared to the higher speed.

### 4.3.3 Drag mode

In thrust mode, when the e-machines of the test vehicle drive the belts of the test stand, it is difficult, or without special measuring technology even impossible, to distinguish the loss share of the transmission, wheels and tyres. Therefore, to determine the losses in the individual components, measurements in drag mode are required. In addition, the drive shafts are removed in the second step so that there would be no longer any connection

between the wheels and the transmission. Thus, while the engine of the test bench puts the drive train of the vehicle in motion, its torque direction changes. That would mean different results compared to the thrust mode. Both types of transmission have load related losses which are the main issue between drag and thrust mode. The load losses are intended to be constant under different temperatures. For multi-stage transmissions, differences would result. Nevertheless, for the transmissions of the test vehicle, the differences are negligible. That is why a comparison with the values under load is permissible. Without drive shafts, the test bench only must move the wheels and wheel bearings. The power differences cause the losses that occur in the transmission and by the rotating shaft of the electric motor.

In the course of this thesis, a simple driving curve was developed for the drag tests. This can be seen in Figure 22.

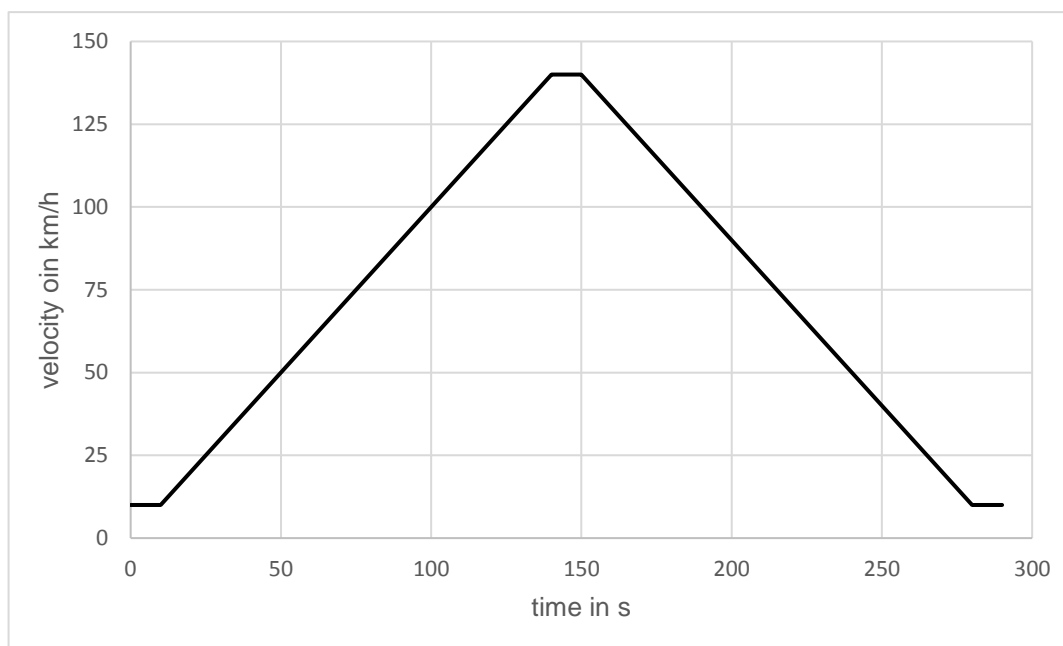


Figure 22. Driving profile in drag mode

A cycle begins with a run of ten seconds at the constant speed of 10 km/h. Then the dynamometer accelerates the speed by 1 km/h/s, so that after 130 s a speed of 140 km/h is reached. This is then maintained constant for ten seconds. Finally, the dynamometer delays the speed by 1 (km/h)/s, so after 130 s, the initial speed of 10 km/h is reached again. This is repeated immediately.

At the same time, the temperature of the test rig is slowly increased to observe the different behaviour at different temperatures. Figure 23 illustrates this temperature curve.

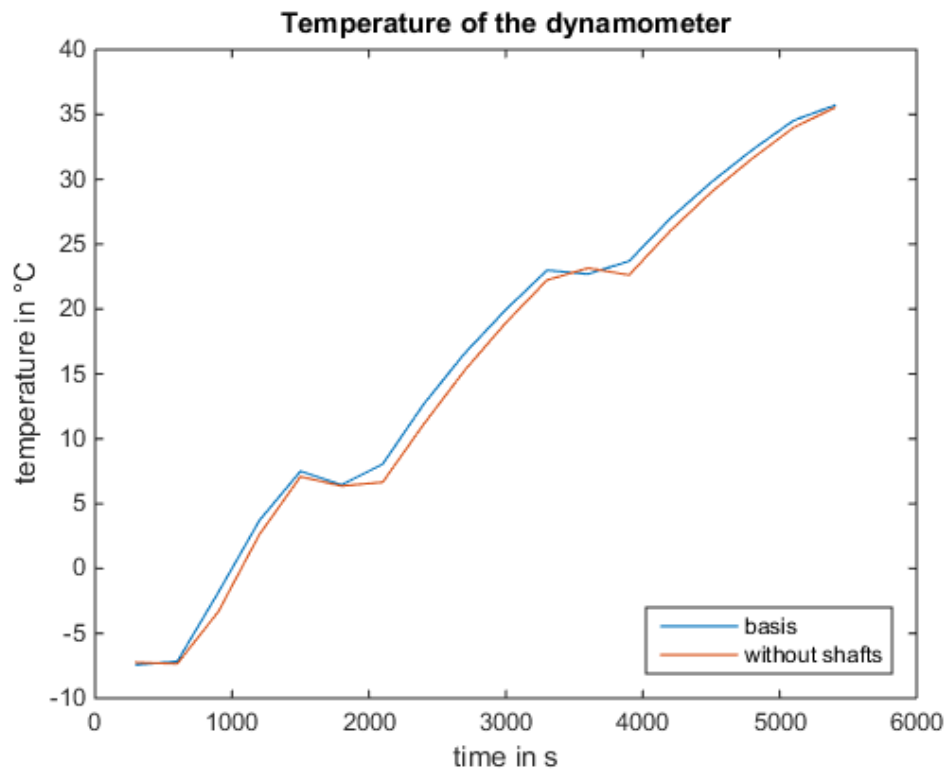


Figure 23. Temperature of the dynamometer in drag mode

The chamber was cooled overnight to -7 °C. This temperature is held for ten minutes after starting the measurements. The new set point temperature is then +7 °C. The climate system of the test bench now adjusts the actual temperature. This is then maintained again for ten minutes. Thereafter, this process is repeated with the two other set point of temperatures 23 °C and 35 °C.

## 5 ANALYSIS OF THE RESULTS

This chapter first evaluates the results of the measurements and after that in the first step, the test with a constant speed are considered because it is easier to formulate general statements in the stationary state. In the second step, the measurements in the WLTC allow the investigation of the dynamic behaviour of the components.

This is followed by a brief examination of the errors made and other potential errors related to the measurement technology. The chapter concludes by comparing the measurement results with each other in view of the driving range.

### 5.1 Evaluation of the data

The actual total energy demand is determined by the power drawn from the battery. In addition to the CED described in Chapter 3, this includes the energy required for the auxiliary systems and the battery management system.

The aerodynamic drag is calculated under the influence of the measured speed. Likewise, the acceleration resistance is calculated considering the measured acceleration. The values used for the power loss of EM1 and EM2 (including losses for power electronics) are direct measured values of the CAN system of the vehicle. The battery power results from the current and voltage measured at the battery output. In order to represent the engine power, the electrical power of the two electric motors is added. As mentioned in Chapter 4.3.3, when measuring in thrust mode, it is not possible to separate the power dissipating the losses caused by the transmission, wheel bearing and rolling resistance. That is why they are collectively presented. They result from the difference between engine power and losses of electric motors and driving resistances.

In this chapter, two kinds of figures were used to represent the energy demand. In the measurements at constant speed, instead of energy, power is shown. In contrast, WLTC measurements show energy demand as an area. Here the power is shown as the gradient of the line.

### 5.1.1 Stationary state

**This content is protected by AUDI AG**

### 5.1.2 Drag mode

In Chapter 4.3.3, the exact measurement process, which leads to the results in this section, was described in detail. As described in this chapter, in drag mode the test bench drives the vehicle. The measurements indicate negative forces. This means that in the interpretation of the diagrams, the higher a value or a line is, the lower is the acting force. The evaluation takes place here on the basis of the respectively acting forces in the phases of the constant speeds of 10 or 140 km/h. The illustrated lines are, in fact, points with interpolated connections.

Figure 31 shows that the drag force at 10 km/h at the beginning of -7 °C is slightly more than twice as high as at the end of the test run at 35 °C chamber temperature. The values at 140 km/h show a very similar picture.

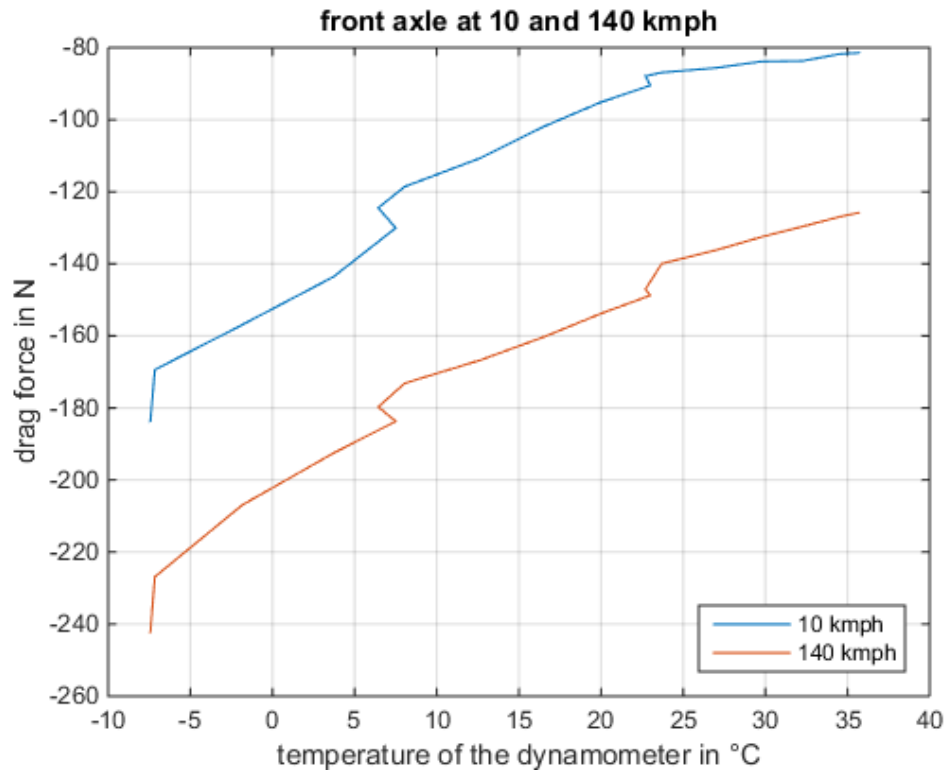


Figure 24. Comparison 10 km/h and 140 km/h

The difference between the forces required for 10 km/h and 140 km/h driving speeds remains the same over the temperature range.

The values at similar x-values are given by the temperature profile since the target temperature is maintained for ten minutes each.

A more accurate localization of the losses can be made if one compares the measurement with and without shafts.

In Figure 32, the blue line, here referred to as "basis", represents the drag measurement in mode "N" (neutral). The red line shows the measurement without shafts.

Range 1 thus only shows the influence of wheels, tyres and wheel bearings.

The difference between the blue and the red line (range 2) represents the loss caused by transmission and the rotation of the motor shaft.

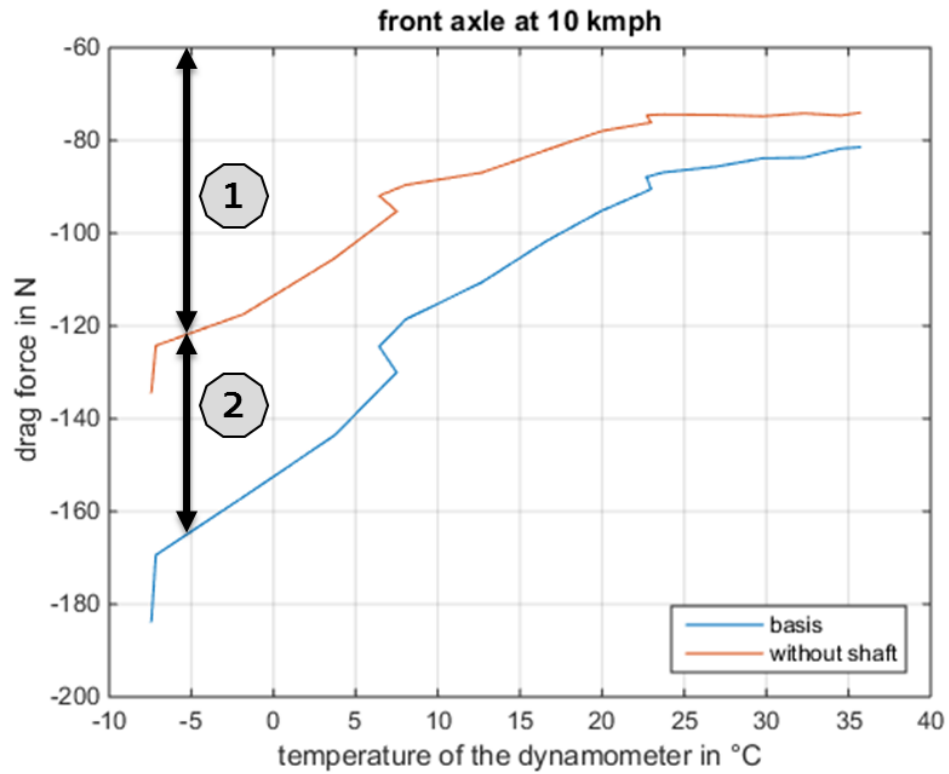


Figure 25. Drag force at 10 km/h on the front axle

In addition to the fact that the losses are reduced when the chamber becomes warmer, the temperature behaviour of the transmission is different than of the wheels and tyre area. The blue line representing the influence of transmission and motor has a steeper slope. As a result, this fraction is at approximately 10 N at 35 °C.

The difference between the curves, as shown in Figure 33, illustrates that the losses in the transmission and the electric motor decrease with increasing temperature in all tested cases.

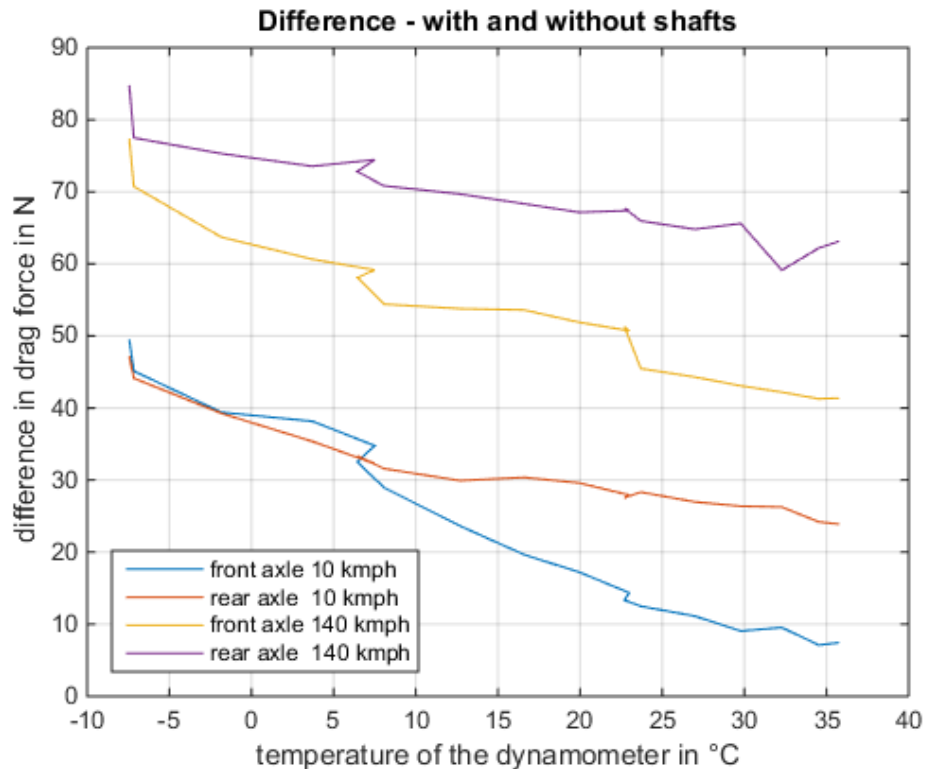


Figure 26. Differences between the test with and without shafts

At 10 km/h, the losses on the front and rear axle are identical at the beginning. At the higher speed, a difference occurs starting at the beginning. The difference remain larger on the rear axle compared to the front axle regardless of the speed. As it can be seen in the Figure 33, the losses on the front axle at 10 km/h at 35 °C are almost negligible, while on the rear axle they are circa three times larger. If the difference between the axles at the beginning was about 10 N, it has nearly doubled at the end.

When this is reflected on the temperature curves of the transmission oil as described in Chapter 5.1.1, a reason can be suggested: the transmission on the front axle becomes warmer. Due to the higher viscosity of the transmission oil with increasing temperature, lower losses are achieved.

One possible reason for this is the better isolation of the front transmission and its location in the car. In the front area of the vehicle, there are in total more components and an extra support frame installed, so that this transmission is less subject to the air flow than the one on the rear axle.

Based on this, one can recognize the great importance of the steady-state temperatures.

### 5.1.3 Steady-state temperatures

**This content is protected by AUDI AG**

### 5.1.4 Unsteady state – WLTC

**This content is protected by AUDI AG**

### 5.1.5 Impact of auxiliary systems on the driving range

**This content is protected by AUDI AG**

## 5.2 Impact on the driving range

Based on the energy consumption, the range of the vehicle can be calculated. As the range or consumption per kilometre in daily usage is the more commonly used term, the summary of results in this section are based on these values.

Consumption is calculated by the energy consumption of the battery divided by the distance travelled.

The range is obtained by dividing the total capacity of the battery by the energy consumption.

$$\text{consumption} = \frac{\text{total energy battery}}{\text{distance}} = \frac{E_{\text{batt}}}{\text{dis}} \text{ in Wh/km} \quad 5.1$$

$$\text{driving range} = \frac{\text{capacity battery}}{\text{consumption}} \text{ in km} \quad 5.2$$

**This content is protected by AUDI AG**

## 5.3 Description of errors

In this thesis, multiple current signals were used to calculate electrical power. These fluctuate very strongly and with a very high frequency. By calculations like addition or division of these signals, deviations occur quickly. The current measurement technology causes deviations. In addition to the inaccuracies of the measurement technique another error results by the driving robot. This drives the cycle curve within a certain tolerance range. The robot acts like an automatic controller, which means it brakes and accelerates all the time to maintain the set point velocity. The velocity signal has a measurement accuracy of 0.1 km/h.

For organizational reasons, the measurements at 30 km/h of constant speed could not complete the conditioning to the outside temperature. Thus, the starting temperature of the components was sometimes significantly higher. Of course, this leads to falsified loss values. Moreover, the sensors for the tyre temperatures were slightly incorrectly calibrated. This results in a difference between measurement signal and real-life value of circa 2-3 K. In addition, there is a slight deviation in the measurement process. For example, a delayed start of the measured value recording shifts the power and energy curve, making it more difficult to compare. At some points of the evaluation, this offset could not be excluded.

Overall, these errors were the same in all tests made. Because mainly differences and relative data were used in this thesis, these errors can be considered negligible. Nonetheless, when looking at the absolute values, these errors need to be taken into account.

## 6 SUMMARY AND OUTLOOK

Overall, it can be said that the driving range of a Battery Electric Vehicle depends highly on the outside temperature.

The differences arise, on the one hand, from the changed driving resistances and, on the other hand, through the losses in the drive train. In addition, there is a strongly varying energy demand for secondary consumers such as the Battery Management System. The losses in the e-machines and the associated power electronics are altogether significantly less dependent on the outside temperature than the transmission since these components have their own cooling systems. A measure for reducing these losses would accordingly be an optimization of these cooling systems or a change in their settings. Thus the potential for a better driving range could be better exploited by the improved efficiency of the electric machines at cool temperatures. The losses in the transmission, however, result in a different behaviour. The warmer the transmission, the lower the losses. Moreover, the results of this thesis show a difference in losses in the transmissions on the front and rear axles.

The front transmission is in many cases warmer than the rear. This can largely be attributed to the position within the vehicle. At the current version of the sample vehicle, nearly no isolation is in use. There are some methods to avoid the airflow hitting the components. This means that even by simple structural measures, the efficiency of the transmission could be improved. Thus, a higher operating temperature could be achieved by insulating mats around the e-machine/transmission complex. Another measure that would bring, with a relatively small effort, lower transmission losses and thus higher driving ranges, is the use of a different gear oil. In particular, good viscosity properties at low temperatures would be advantageous.

If these measures are ineffective, one option could be to use the energy that is generated during recuperation to heat the transmission oil. Nonetheless, this would mean that less recuperation energy comes as input to the battery and can be used for other purposes. Whether this idea can bring any real benefit, and if so, at what outside temperatures, should be further investigated.

Nevertheless, the differences between transmissions could partly result from their different construction methods.

It must be further examined which gearbox effectively offers the better efficiency, and which influence the type of oil and thus its heat capacity has on the losses.

As a whole, based on the steady-state temperatures and also the final temperatures of the various phases of the WLTC, it can be seen that the generally transmissions heat up quite quickly. Even at very low outside temperatures, the temperature of the oil rises in the test at the speed of 60 km/h and in the WLTC tests into the same temperature window, which minimizes the loss differences.

## 7 REFERENCES

- [1] acatech – Deutsche Akademie der Technikwissenschaften e.V. *Nationale Plattform Elektromobilität. Hintergrund - Die Ziele.* <http://nationale-plattform-elektromobilitaet.de/hintergrund/die-ziele/>. Accessed 18 January 2019.
- [2] Audi of America. 2019. *Audi e-tron.* <https://www.audiusa.com/models/audi-e-tron>. Accessed 18 January 2019.
- [3] Bargende, M., Reuss, H.-C., and Wiedemann, J., Eds. 2018. *Nutzungsorientierte Auslegung des Antriebsstrangs und der Reichweite von Elektrofahrzeugen.* Wissenschaftliche Reihe Fahrzeugtechnik Universität. Springer Vieweg, Stuttgart.
- [4] Bizzarri, A. 2018. *Thermal management for batterie in E-mobility applications.*
- [5] BMWi. 2018. *Electric mobility in Germany.* <https://www.bmwi.de/Redaktion/EN/Dossier/electric-mobility.html>. Accessed 18 December 2018.
- [6] BMWi. 2018. *Ready for the next phase of the energy transition.* <https://www.bmwi.de/Redaktion/EN/Dossier/energy-transition.html>.
- [7] Ersoy, M. and Gies, S., Eds. 2017. *Fahrwerkhandbuch.* Springer Fachmedien, Wiesbaden.
- [8] Füßel, A. 2017. *Technische Potenzialanalyse der Elektromobilität.* Springer Fachmedien, Wiesbaden.
- [9] Giffi, C. A., Vitale Jr, J., Schiller, T., and Robinson, R. 2017. *A reality check on advanced vehicle technologies. Evaluating the big bets being made on autonomous and electric vehicles.*
- [10] 2017. *Global WLTP roll-out for more realistic results in fuel consumption. Questions and answers regarding the new international test procedure,* Berlin.
- [11] Grote, K.-H., Bender, B., and Göhlich, D., Eds. 2018. *Dubbel. Taschenbuch für den Maschinenbau.* Springer Vieweg, Wiesbaden.
- [12] Hoese, F. 2011. *Getrag BEV Demonstrator (2010).* <https://www.automativ.de/getrag-bev-demonstrator-2010-id-30185.html>. Accessed 18 January 2019.

- [13] Knischourek, E., Mühlbauer, K., and Gerling, D. 2019. *Reduktion der Batteriekapazität in Elektrofahrzeugen durch Wirkungsgradsteigerung des elektrischen Antriebsstranges*, München.
- [14] Köbler, J. 2018. *The people behind the Audi e-tron. #3 High Voltage. Encounter 2*, Ingolstadt.
- [15] Leitinger, C. and Dr.-Ing. Brauner, G., Eds. 2008. *Elektrische Mobilität – Effizienzsteigerung sowie Herausforderungen für die Energiebereitstellung*.
- [16] Liebl, J., Lederer, M., Rohde-Brandenburger, K., Biermann, J.-W., Roth, M., and Schäfer, H. 2014. *Energiemanagement im Kraftfahrzeug. Optimierung von CO<sub>2</sub>-Emissionen und Verbrauch konventioneller und elektrifizierter Automobile*. Springer Vieweg, Wiesbaden.
- [17] Pischinger, S. and Seiffert, U., Eds. 2016. *Vieweg Handbuch Kraftfahrzeugtechnik*. Springer Fachmedien, Wiesbaden.
- [18] Schaeffler AG. 2018. *Dual Drive Provides Comfort and Driving Pleasure*. [https://www.schaeffler.com/content.schaeffler.com/en/news\\_media/press\\_office/press\\_releases/press\\_releases\\_detail.jsp?id=85269120](https://www.schaeffler.com/content.schaeffler.com/en/news_media/press_office/press_releases/press_releases_detail.jsp?id=85269120). Accessed 18 January 2019.
- [19] Seidel, T. 2015. *Reibmomentmessung Radlager*, Braunschweig.
- [20] Société de Technologie Michelin, F-Clermont-Ferrand. 2005. *Der Reifen - Rollwiderstand und Kraftstoffersparnis. Wie Reifen Kraftstoffverbrauch und Emissionen senken können*, Karlsruhe.
- [21] Subramonium A K, N., Shetty, P., Saravanan, G., and Vivekanandan, S. 2017. Technology and Key Strategy of IE4 Permanent Magnet Brushless DC Motor Drive for Electric Vehicle Application. *Int. Journal of Engineering Research and Application*, 7, 25–31.
- [22] Tesla, I. 2019. *Range per Charge Model S*. [https://www.tesla.com/en\\_GB/models?redirect=no](https://www.tesla.com/en_GB/models?redirect=no). Accessed 18 January 2019.
- [23] Trezesniowsik, M., Ed. 2017. *Fahrwerk*. Handbuch Rennwagenteknik. Springer Fachmedien, Wiesbaden.
- [24] Tschöke, H. 2015. *Die Elektrifizierung des Antriebsstrangs*. Basiswissen. Springer Fachmedien, Wiesbaden.
- [25] VDI Wissensforum GmbH, Ed. 2018. *Dritev. Drivetrain for Vehicles; EDrive; Transmissions in mobile machines*. International VDI Congress. VDI Berichte 2328. VDI Verlag GmbH, Düsseldorf.

**LIST OF SYMBOLS**

<b>Symbol</b>	<b>Explanation</b>	<b>Unit</b>
P	Power	W
R	ohmic resistance	$\Omega$
I	current	A
$\tau$	shear stress	$\text{N/m}^2$
$\dot{\gamma}$	shear rate	-
$\eta$	dynamic viscosity	$\text{Ns/m}^2$
A, b	parameters	-
$M_x$	torque	Nm
$\mu$	friction coefficient	-
F	force	N
d	diameter	m
E	energy	J
dis	distance	m
m	mass	kg
a	acceleration	$\text{m/s}^2$
$\varepsilon$	factor rotational mass	-
f	parameter	-
g	acceleration of gravity	$\text{m/s}^2$
$\alpha$	road gradient	$^\circ$
v	velocity	m/s
$A_x$	cross-sectional area	$\text{m}^2$
$c_d$	air resistance coefficient	-
$\rho$	air density	$\text{kg/m}^3$
p	ambient pressure	Pa
M	molar mass of air	kg/mol
R	universal gas constant	$(\text{kg}\cdot\text{m}^2)/(\text{s}^2\cdot\text{mol}\cdot\text{K})$
T	temperature	K
U	voltage	V
n	rotation speed	1/min
CED	cycle energy demand	Wh

**LIST OF FIGURES**

Figure 1. Driving range per charge at -10 °C, calculator by Tesla [22]	7
Figure 2. Driving range per charge at 20 °C, calculator by Tesla [22]	7
Figure 3. Comparison losses in the powertrain of a ICEV and a BEV (own diagram based on [15])	9
Figure 4. Illustration of the topology	12
Figure 5. Operating temperature of a lithium ions battery [4]	13
Figure 6. Bridge circuit [13]	14
Figure 7. Sectional view electric machine front axle [2]	16
Figure 8. Speed-torque characteristics of an ASM motor [21]	17
Figure 9. Sectional view of the axis parallel (left) and coaxial (right) transmission of the sample vehicle [18]	19
Figure 10. The different generations of wheel bearings [7]	20
Figure 11. Exploded view of a wheel carrier [2]	21
Figure 12. Friction moment of a wheel bearing at 0 °C and 20 °C ambient temperature [19]	22
Figure 13. Rolling resistance depending on the ambient temperature, own translation of [20, p. 86]	24
Figure 14. Power demand for the auxiliary energy flow with and without preconditioning (dashed) of the passenger cabin [25]	25
Figure 15. Driving resistances	26
Figure 16. Aerodynamic drag $F_{dr}$ as a function of the ambient temperature	28
Figure 17. Aerodynamic drag $F_{dr}$ as a function of the velocity $v$ (basis $v = 100$ km/h)	28
Figure 18. Schema of a flat-bed test bench	30
Figure 19. Measurement technology on the rear axle	31
Figure 20. Driving profile of the WLTC	33
Figure 21. Driving profile at constant speed 30 km/h (dashed) and 60 km/h	34
Figure 22. Driving profile in drag mode	35
Figure 23. Temperature of the dynamometer in drag mode	36
Figure 31. Comparison 10 km/h and 140 km/h	39
Figure 32. Drag force at 10 km/h on the front axle	40
Figure 33. Differences between the test with and without shafts	41

**APPENDICES**

**Appendix 1 - Test preparation**

